

# Time delay induces a back to back Hopf bifurcation on oncolytic virotherapy.

Dong-Hoon Shin

Department of Global Finance and Banking, Inha University, Incheon 22212, Korea

## Abstract

*This study analyzes a basic mathematical model for the dynamic interactions among tumor cells, infected tumor cells and viruses population, focusing on the viral lytic cycle for oncolytic virotherapy. I study the time delay effect of viral infection on tumor cell populations by identifying bifurcation thresholds in both the burst rate and time delay of viral infection in oncolytic virus therapy. Time delay plays an important role in changing the structure of tumor cell populations in a dynamical system. The multi-bifurcation thresholds of the time delay are observed and also dependent on the bursting rate. This study demonstrates a strong relationship between viral burst rates and time delays in population dynamics. The results of this study show that time delay affects oscillation generation and results in back-to-back Hopf bifurcation. This study provides insight into understanding the relationship between the two control parameters, in which tumor cell populations pattern from equilibrium steady-state solutions to periodic solutions and from periodic solutions to equilibrium-state solutions.*

**Keywords:** Computational biology; oncolytic virotherapy; bifurcation; dynamical system

## 1. Introduction

Oncolytic viruses are genetically modified viruses that can infect and multiply cancerous cells, but leave normal, healthy cells intact. Oncolytic viruses can be divided into two types: oncolytic wild viruses, which occur naturally and preferentially in human cancer cells, and genetically modified viruses engineered to achieve selective oncolysis. Wild-type viruses have shown limited oncolytic potency in some preclinical trials, whereas transgenic viruses appear to have large oncolytic potency (Kirn & McCormick (1996), Kaplan (2005), Roberts, et. al. (2006)). Prior to the 1990s, case studies and small-scale experiments with various viruses in cancer treatment were reported (Chiocca (2002)). Genetic engineering began to be used for oncolytic viruses in the 1990s (Martuza, et. al. (1991)). To date, many types of viruses have been modified for experiments (Lawler et. al. (2017)), and some oncolytic viruses have been approved for human clinical trials (Maroun, et. al. (2017)). However, the potential of oncolytic viruses does not seem to have been reached yet (Chiocca & Rabkin (2014)). One major challenge is how to fully spread the virus into solid tumors (Mok, et. al. (2009)).

An understanding of the dynamics of spread of oncolytic viruses through tumors can help overcome these difficulties and develop strategies for clinical application. Mathematical modeling can explore the full spectrum of possible outcomes and provide a basis for optimizing treatment. Several attempts have been made to understand and characterize viral dynamics with mathematical models. See Bajzer, et. al. (2008), Friedman, et. al. (2006), Wodarz (2001) and Wu, et. al. (2001) for example. These mathematical models can be roughly divided into two classes. One class uses Ordinary Differential Equations (ODEs), including Delay Differential

## ***Time delay induces a back to back Hopf bifurcation on oncolytic virotherapy.***

Equations (DDEs) (Novozhilov, et. al.(2006), Karev, et. al.(2006), Wodarz & Komarova (2009), and Wang, et. al.(2013)) and the other class uses Partial Differential Equations (PDEs) (Friedman, et. al.(2006), Wein, et. al.(2003) and Wu, et. al.(2001)). For PDE models of oncolytic virus therapy, most use the idea of fluid dynamics to model solid tumor growth in which tumor cells convect in fluid velocity fields within the tumor and the virus simply spreads within the tumor. All these modeling studies have provided specific insights into viral treatment. A study by Jain and colleagues in particular highlights the importance of the spreading properties of viruses(Mok, et. al.(2009)). However, it is well known that the growth of solid tumors, especially brain tumor gliomas, also exhibits characteristics of cell proliferation (Harpold, et. al.(2007)).

The viral lytic cycle is the duration of the viral life cycle within a cell, starting from the moment the virus enters the cell and ending when a certain number (viral burst size) of newly replicated virus emerges upon cell lysis. It is an important parameter of viral dynamics. Wang, et. al.(2013) is the first to incorporate the viral lysis cycle as a delay parameter in a mathematical model for oncolytic virus therapy. In this paper, we aim to analyze the effect of time delay of the virus infection on oncolytic virotherapy. Our numerical results show there is a strong relationship between the virus bursting size and the time delay in the generation of oscillations. This paper is structured as follows. Section 2 reviews models of the dynamics of oncolytic viruses with basic equations and introduces common basic models. In addition, equilibrium analysis and stability are reviewed, and conditions of numerical simulation are checked. In Section 3, we investigate the effect of time delay on the dynamics of the tumor cell population through a basic model. We can know that the bifurcation value in the bursting rate depends on a time delay. Finally, in conclusion, we summarize our results and we highlight that time delay affects oscillation generation.

## **2. Materials and Methods**

### **2.1 Model**

The OV model is a three dimensional

$$\begin{aligned} \frac{dx}{dt} &= k_1x \left(1 - \frac{x+y}{K}\right) - k_2xz \\ \frac{dy}{dt} &= k_2x(t-\tau)z(t-\tau) - \delta_1y \\ &(1) \\ \frac{dz}{dt} &= k_3y - k_2xz - \delta_2z \end{aligned}$$

where  $x(t)$ ,  $y(t)$  and  $z(t)$  represent populations of tumor cells, infected tumor cells and free viruses, respectively. The  $k_1$  is the proliferation rate of tumor cell and  $K$  is the carrying capacity of a tumor. The term  $k_1x \left(1 - \frac{x+y}{K}\right)$  explains the logistic growth rate of a tumor cell population  $x(t)$ . The constant value  $k_2$  is the infection rate of the virus and the term  $k_2xz$  describes the rate of infected tumor cells by free viruses  $z(t)$ .  $\tau$  is a time delay  $\delta_1$  represents the death rate of infected tumor cells. The  $k_3$  is the bursting size of free virus particles. The term  $\delta_2$  is the clearance rate of free virus particles.

For non-dimensionalization, we set  $\tau = \delta_1 t$ ,  $x = K\hat{x}$ ,  $y = K\hat{y}$ ,  $z = K\hat{z}$ . Then

Equation (1) become

$$\begin{aligned} \frac{d\hat{x}}{d\tau} &= \frac{k_1}{\delta_1} \hat{x}(1 - \hat{x} - \hat{y}) - \frac{k_2 K}{\delta_1} \hat{x}\hat{z} \\ \frac{d\hat{y}}{d\tau} &= \frac{k_2 K}{\delta_1} \hat{x}\hat{z} - \hat{y} \\ (2) \\ \frac{d\hat{z}}{d\tau} &= \frac{k_3}{\delta_1} \hat{y} - \frac{k_2 K}{\delta_1} \hat{x}\hat{z} - \frac{\delta_2}{\delta_1} \hat{z} \end{aligned}$$

We have the following model by setting the parameters;  $a = \frac{k_1}{\delta_1}$ ,  $b = \frac{k_2 K}{\delta_1}$ ,  $c = \frac{k_3}{\delta_1}$  and  $d = \frac{\delta_2}{\delta_1}$

$$\begin{aligned} \frac{dx}{dt} &= ax(1 - x - y) - bxz \\ \frac{dy}{dt} &= bx(t - \tau)z(t - \tau) - y \\ (3) \\ \frac{dz}{dt} &= cy - bxz - dz \end{aligned}$$

All parameters are described in Table 1.

**Table 1. Non-dimensionalized model parameters.** All parameters are assumed to be non-negative.

Parameter	Description	Component
$a$	Proliferation rate of tumor cell	$a = \frac{k_1}{\delta_1}$
$b$	Infection rate of virus into tumor cell	$b = \frac{k_2 K}{\delta_1}$
$c$	Bursting size of virus	$c = \frac{k_3}{\delta_1}$
$d$	Clearance rate of free virus particles	$d = \frac{\delta_2}{\delta_1}$

## 2.2 Analysis and Stability of Equilibrium

For  $\tau = 0$  (no time delay in virus infection), there exist three equilibrium points; two equilibrium solutions  $E_0(0, 0, 0)$  and  $E_1(1, 0, 0)$  in the positive invariant domain D and the other one  $E_2(x^*, y^*, z^*)$  in either the negative or the positive domain depending on the parameter values.

$$E_2(x^*, y^*, z^*) = \left( \frac{d}{b(c-1)}, \frac{ad(bc-b-d)}{b(c-1)(bc-b+ad)}, \frac{a(bc-b-d)}{b(bc-b+ad)} \right)$$

Using the linear stability analysis,  $E_0(0, 0, 0)$  is always unstable equilibrium point.  $E_1(1, 0, 0)$  is a stable point if  $a \leq \frac{d}{c-1}$ . Otherwise,  $E_1(1, 0, 0)$  is an unstable equilibrium point.  $E_2(x^*, y^*, z^*)$  is stable if  $p_i > 0$ ,  $i=1, 2, 3$  and  $p_1 \cdot p_2 > p_3$ , where  $p_i$  is the coefficient of the characteristics equation  $P = \lambda^3 + p_1\lambda^2 + p_2\lambda + p_3$ , where

$$p_1 = \frac{bc + ad + bcd - b}{b(c-1)},$$

$$p_2 = \frac{ad(cd + c - 1)}{b(c-1)^2} + \frac{ad(bc - b - d)(a - d)}{b(c-1)(bc - b + ad)},$$

$$p_3 = \frac{ad(bc - b - d)}{b(c-1)}$$

For  $\tau \neq 0$ , we refer to Wang, et. al.(2013)

### 2.3 Numerical Simulation

We used the Runge-Kutta 2nd order method15 to compute the numerical solutions in MATLAB (The Mathworks, Natick, MA). The small-time step  $\Delta t = 0.05$  was used to check the accuracy of the numerical method. For numerical simulations, we set the parameters  $a = 0.31$  (growth rate of cancer cell from the experimental data) and  $d = 0.44$  with initial conditions  $x(0) = 0.5$ ,  $y(0) = 0$ , and  $z(0) = 1.5$ . Both the infection rate ( $b$ ) and the bursting rate of virus ( $c$ ) are considered as variables.

## 3. Results

### 3.1 The effect of a time delay on the dynamics of tumor cell population

We investigated the effect of the time delay on the tumor cell population. We set the busting rate ( $c = 5$ ; different values of  $c$  will be discussed later) and computed the tumor cell population over time for  $\tau = 0, 5$  and  $10$ . Without the delay time, the tumor cell population converges to equilibrium value  $0.215$ . However, for  $\tau = 5$ , the tumor cell population exhibits oscillations over time. For  $\tau = 10$ , the amplitude of oscillations reduced. If the delay time is higher (longer), then the result is the same as the result at  $\tau = 0$  (Figure 1). Our numerical result indicates that there is a Hopf bifurcation where the structure of the tumor cell population changed at a certain  $\tau = \tau^*$  from steady state to periodic solutions and suggests that the time delay  $\tau$  can be a bifurcation parameter on the dynamics.

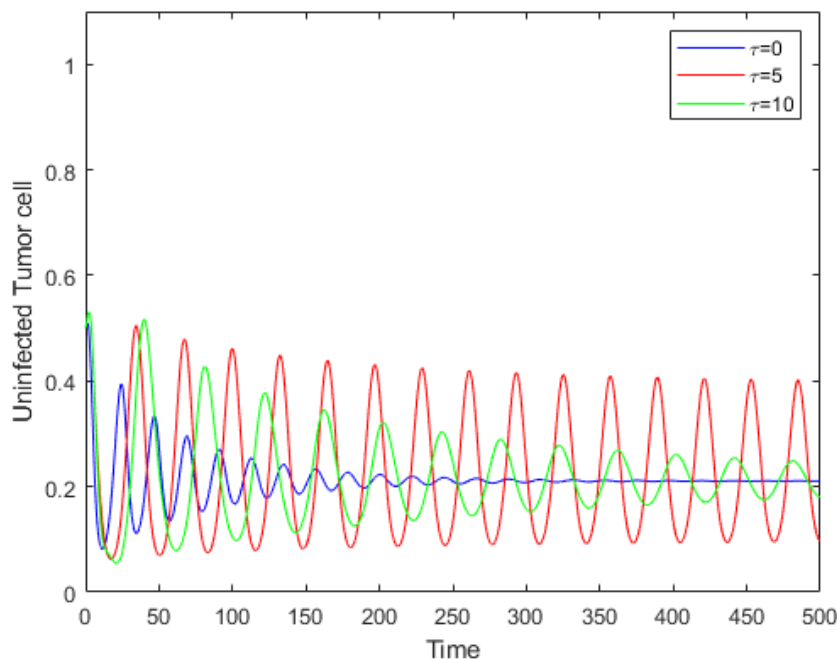
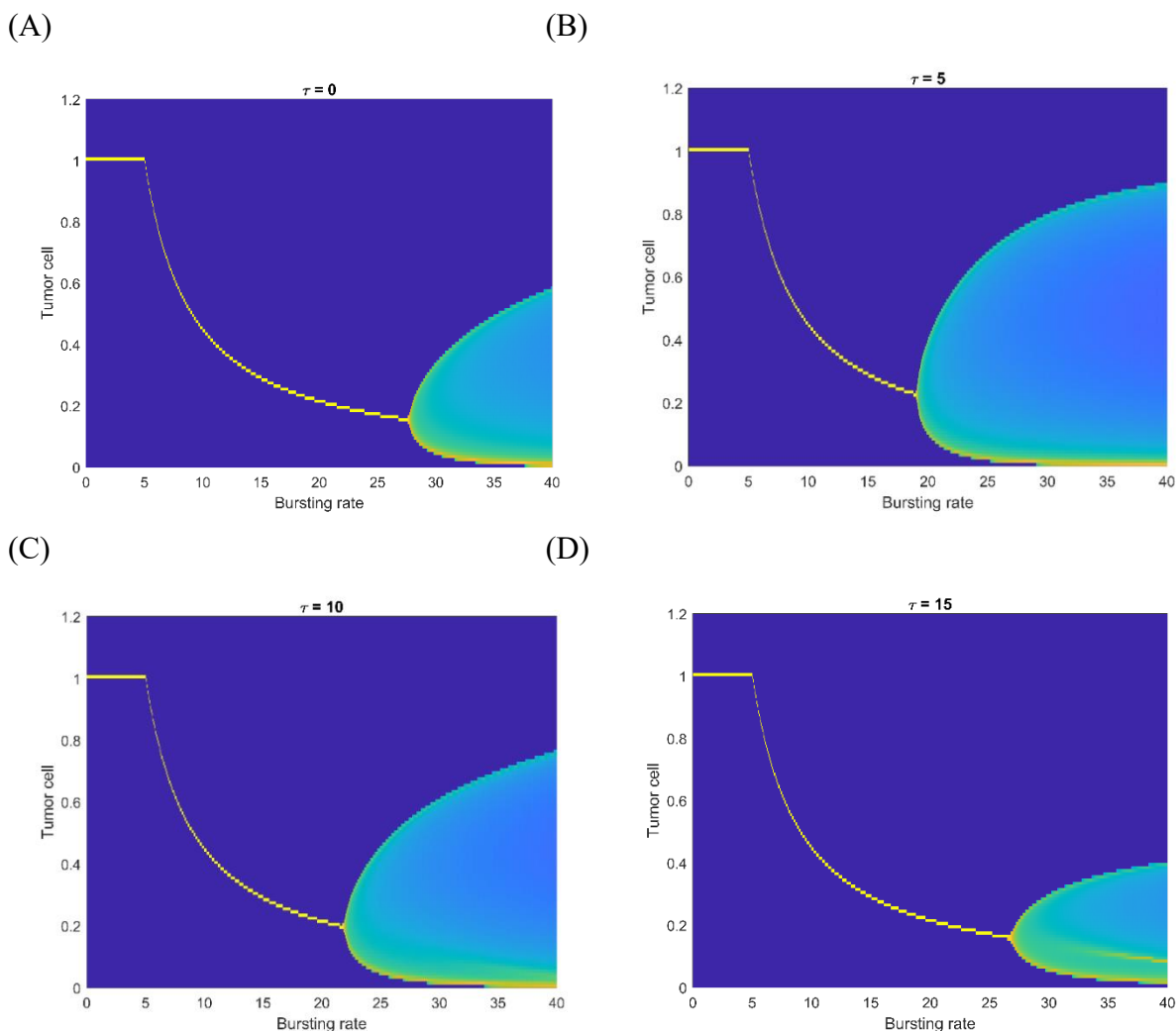


Figure 1: **The effect of a time delay on tumor cells population.** Time series of uninfected tumor cell population for different values of  $\tau$ . The tumor cell population shows a damped oscillation for  $\tau = 0$ . However, it displays a periodic solution (oscillation) for  $\tau = 5$  and back to damped oscillations for  $\tau = 10$ . Parameters used were  $a = 0.31$ ,  $b=0.11$ ,  $c = 5$  and  $d = 0.44$ .

### 3.2 The bifurcation value in the bursting rate depends on a time delay.

The changes in the stability of an equilibrium depend on parameters. This qualitative changes in a dynamic structure is called bifurcation. Figure 2 shows bifurcation diagrams of equilibrium tumor cell population over the bursting rate. We calculated the equilibrium tumor cell population over time for each bursting rate ranged from 0 to 40 with step size 0.01. Our model exhibits two bifurcation values in the bursting rate at  $c = c_1^*, c_2^*$ . There is a transcritical bifurcation at  $c = c_1^*$  where the equilibrium point  $E_1(1, 0, 0)$  is stable and  $E_2(x^*, y^*, z^*)$  is unstable for  $0 \leq c < c_1^*$ . However, the stability of equilibrium points changes at  $c = c_1^*$  where  $E_1(1, 0, 0)$  becomes unstable and  $E_2(x^*, y^*, z^*)$  is stable for  $c > c_1^*$ . A Hopf bifurcation occurred at  $c = c_2^*$  where the equilibrium point  $E_2(x^*, y^*, z^*)$  is stable spiral for  $c_1^* < c < c_2^*$  but there is a limit cycle around the equilibrium point and the tumor cell population shows oscillation for  $c > c_2^*$ . For  $\tau = 0$ , we found  $c_1^* = 5$  and  $c_2^* = 27$  (Figure 2A). Interestingly, Hopf bifurcation value ( $c_2^*$ ) shifts left or right depending on a time delay ( $\tau$ ) (Figure 2B, 2C, 2D).



**Figure 2: Bifurcation diagram with bursting rate with different time delay.** (A)-(D) are bifurcation diagrams for tumor cell population density with respect to the bursting rate with time delay  $\tau = 0, 5, 10$  and  $15$ , respectively. The time delay  $\tau$  induce the second bifurcation threshold value ( $c_2^*$ ). Parameter used were  $a = 0.31, b=0.11, d = 0.44$

### 3.3 Back-to-back Hopf bifurcation with a time delay.

It showed a delay time resulted in shifting of the bifurcation threshold values in bursting rate with different time delays in Figure 2. In this section, we investigated the effect of the time delays on the tumor cell population with different values of bursting rate. We compute the equilibrium density of tumor cell population over time delays ranged from 0 to 100 with step size  $\tau = 0.01$  with fixed values of bursting rate  $c = 18, 19$  and  $20$ . The tumor cell populations exhibit steady state solutions  $x(t) = 0.215$  without a delay time. The tumor cell stays the same equilibrium population when  $c = 18$  in the presence of a delay time of virus infection (Figure 3A). However, it shows oscillations at certain delay times in Figure 3B. The amplitude and the time delay period of oscillations increased as the bursting rate increased (Figure 3C). Our numerical results show that there are multiple of threshold values in delay times at which the equilibrium tumor cell population changes from equilibrium steady state solution to periodic solutions and suggest that there are back-to-back Hopf bifurcation at the threshold values in delay times.

***Time delay induces a back to back Hopf bifurcation on oncolytic virotherapy.***

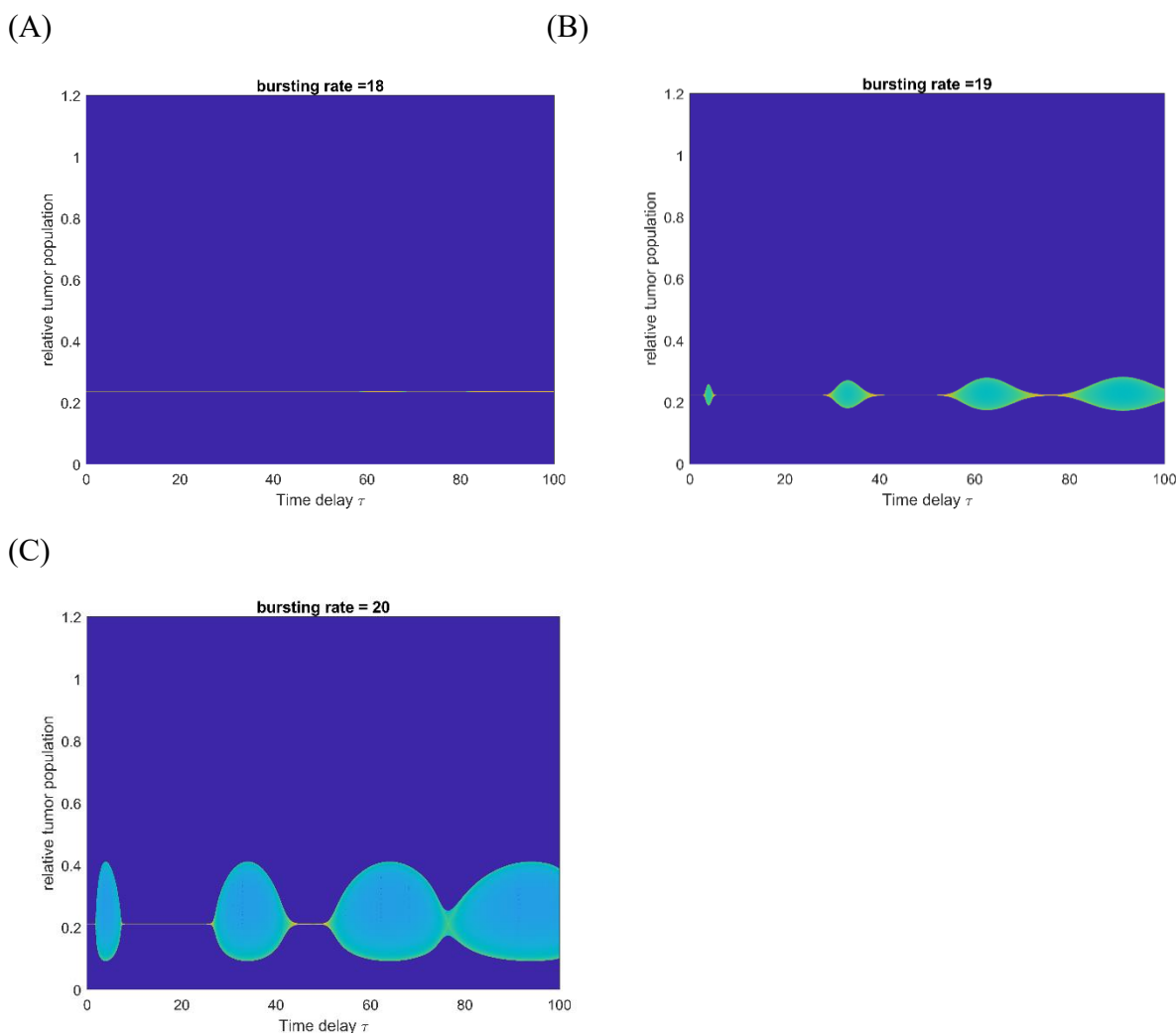
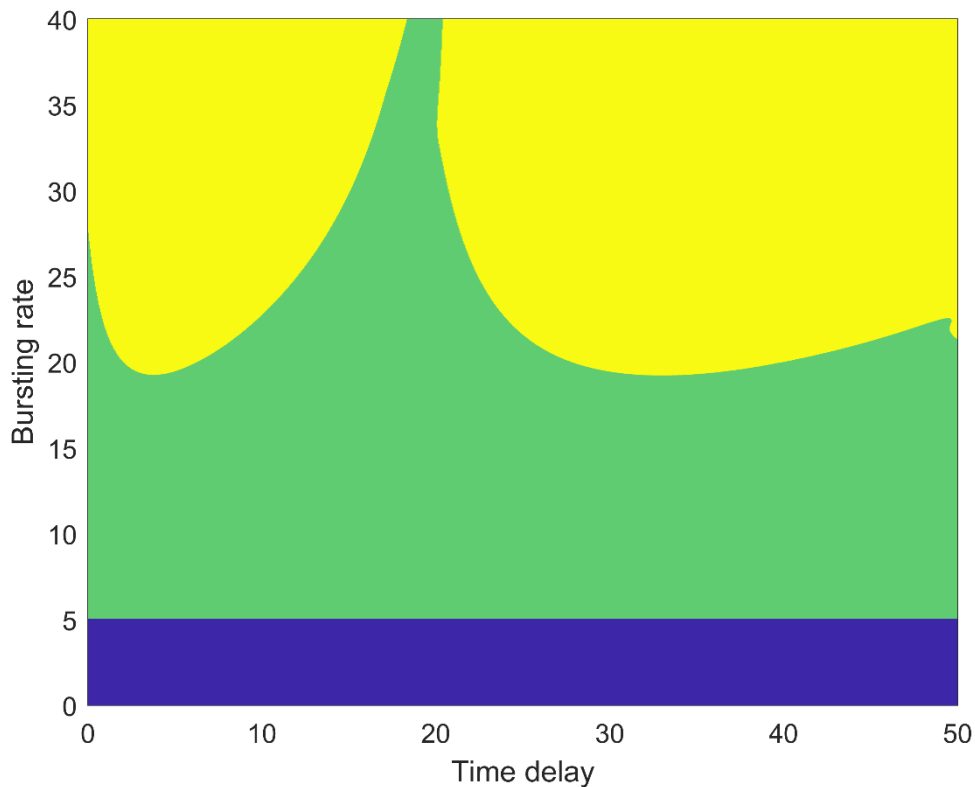


Figure 3: The density of equilibrium tumor cell population when the time delay varies from 0 to 100 with different values of bursting rate. There is no impact of time delay when the bursting rate is 18 (A). The oscillations of tumor cell populations occurred at certain delay times (B and C). We used the parameter  $a = 0.31$ ,  $b=0.11$ ,  $d = 0.44$

The model exhibits two bifurcations with respect to two parameters; the bursting rate and the time delay of the virus infection: Transcritical and Hopf bifurcation. Figure 4 shows the two-dimensional bifurcation diagram. We computed all eigenvalues of Jacobian matrix and identified the stability of equilibrium points when two parameters (bursting rate  $c$  and time delay) vary simultaneously. The Figure 4 shows three different colored regions which represent the following: 1) The blue is the set of parameters  $(\tau, c)$  at which the relative cancer cell population converges to the maximal capacity, 2) the green color indicates that the population exhibits damped oscillations and converges to the population less than the maximal capacity and 3) the yellow colored region is that the population shows oscillations over the time. Our numerical result provides the critical set of values of bifurcation points  $(\tau_1, c_1)$  and  $(\tau_2, c_2)$  which are located on the border between two colored regions. The transcritical bifurcation occurs in between blue and green colored region and the Hopf bifurcation occurs at the border between green and yellow colored region. As shown in Figure 4, the time

## *Time delay induces a back to back Hopf bifurcation on oncolytic virotherapy.*

delay of the virus infection plays an important role in the generation of oscillations when the bursting rate is larger than 20. There are three bifurcation threshold values for  $20 < \text{bursting rate} < 28.2$  where the stability of  $E_2(x^*, y^*, z^*)$  changes either from stable spiral to unstable (limit cycle around the  $E_2(x^*, y^*, z^*)$ ) or unstable to stable spiral, resulting in Hopf bifurcation. Interestingly, there is no effect of the time delay on the tumor cell population if the bursting rate is less than 20.



**Figure 4: Two-dimensional bifurcation diagram for the tumor cell population density;** Time delay on the x-axis, bursting rate on the y-axis. Three colored regions represent the set of two parameters at which three different patterns of tumor cell population over time are observed; the steady-state equilibrium (blue), damped oscillations (green) and oscillations (yellow). Two- bifurcations occurs at the borders between two colors; (1) Transcritical bifurcation on the border between blue and green, (2) Hopf bifurcation on the border between (green and yellow). Parameters used were  $a = 0.31$ ,  $b=0.11$ ,  $d = 0.44$

## **4. Conclusion**

In this paper, we studied the effect of the time delay of the virus infection on the tumor cell population by identifying the bifurcation threshold values in both bursting rate and time delay of virus infection on oncolytic virotherapy. Our numerical results illustrate that there is a strong relationship between the virus bursting rate and the time delay in the population dynamics. The time delay plays an important role in changing the structure of tumor cell populations. Multiple bifurcation threshold values of time delay are observed, and they also depend on the bursting rate. Our numerical results show that the time delay affects the generation of

oscillations: either low bursting rate or high bursting rate. Our result gives an insight into understanding the relationship between two control parameters at which the tumor cell population shows the patterns from equilibrium steady-state solution to periodic solutions and from periodic solutions to equilibrium state solutions. The two-dimensional bifurcation diagram provides a promising result in determining optimal parameters for successful virotherapy.

## **5. References**

1. Bajzer, Ž., Carr, T., Josić, K. (2008). Modeling of cancer virotherapy with recombinant measles viruses. *Journal of theoretical Biology*, 252(1): 109–122. [PubMed: 18316099]
2. Chiocca, E. A. (2002). Oncolytic viruses. *Nature Reviews Cancer*, 2(12): 938. [PubMed: 12459732]
3. Chiocca, E. A., & Rabkin, S. D. (2014). Oncolytic viruses and their application to cancer immunotherapy, *Cancer Immunol Res.* 2(4): 295–00. [PubMed: 24764576]
4. Friedman, A., Tian, J. P., & Fulci, G. (2006). Glioma virotherapy: effects of innate immune suppression and increased viral replication capacity. *Cancer research*, 66(4): 2314–2319. [PubMed: 16489036]
5. Harpold, H. L., Alvord, E.C. Jr, & Swanson, K. R. (2007). The evolution of mathematical modeling of glioma proliferation and invasion. *J Neuropathol Exp Neurol.* 66(1): 1–9. [PubMed: 17204931]
6. Kaplan, J. M. (2005). Adenovirus-based cancer gene therapy. *Current gene therapy*, 5(6): 595–605. [PubMed: 16457649]
7. Karev, G. P., Novozhilov, A. S., & Koonin, E.V.(2006). Mathematical modeling of tumor therapy with oncolytic viruses: effects of parametric heterogeneity on cell dynamics. *Biology direct*, 1(1): 30. [PubMed: 17018145]
8. Kirn, D. H., & McCormick, F. (1996). Replicating viruses as selective cancer therapeutics. *Molecular Medicine Today*, 2(12): 519–527. [PubMed: 9015793]
9. Lawler, S. E., Speranza, M. C., & Cho, C. F. (2017). Oncolytic viruses in cancer treatment: a review. *JAMA oncology*, 3(6): 841–849. [PubMed: 27441411]
10. Martuza, R. L., Malick, A., & Markert, J. M. (1991) Experimental therapy of human glioma by means of a genetically engineered virus mutant. *Science*, 252(5007): 854–856. [PubMed: 1851332]
11. Maroun, J., Muoz-Ala, M., Ammayappan, A., Schulze, A., Peng, K. W., & Russell, S. (2017). Designing and building oncolytic viruses, *Future Virol.* 12(4), 193–13. [PubMed: 29387140]
12. Mok, W., Stylianopoulos, T., Boucher, Y., & Jain, R. K. (2009). Mathematical modeling of herpes simplex virus distribution in solid tumors: implications for cancer gene therapy, *Clin Cancer Res.*, 15(7): 2352–360. [PubMed: 19318482]
13. Novozhilov, A. S., Berezovskaya, F. S., & Koonin, E. V. (2006). Mathematical modeling of tumor therapy with oncolytic viruses: regimes with complete tumor elimination within the framework of deterministic models. *Biology direct*, 1(1): 6. [PubMed: 16542009]
14. Roberts, M. S., Lorence, R. M., & Groene, W. S. (2006) Naturally oncolytic viruses. *Current opinion in molecular therapeutics*, 8(4): 314–321. [PubMed: 16955694]
15. Wang, Y., Tian, J. P., & Wei, J. (2013). Lytic cycle: a defining process in oncolytic virotherapy. *Applied*

*Mathematical Modelling*, 37(8): 5962–5978.

16. Wein, L. M., Wu, J. T., & Kirn, D. H. (2003). Validation and analysis of a mathematical model of a replication-competent oncolytic virus for cancer treatment: implications for virus design and delivery. *Cancer research*, 63(6): 1317–1324. [PubMed: 12649193]
17. Wodarz, D. (2001). Viruses as antitumor weapons: defining conditions for tumor remission. *Cancer research*, 61(8): 3501–3507. [PubMed: 11309314]
18. Wodarz, D., & Komarova, N. (2009). Towards predictive computational models of oncolytic virus therapy: basis for experimental validation and model selection. *PloS one*, 4(1): e4271. [PubMed: 19180240]
19. Wu, J. T., Byrne, H. M., & Kirn, D. H. (2001). Modeling and analysis of a virus that replicates selectively in tumor cells. *Bulletin of mathematical biology*, 63(4): 731. [PubMed: 11497166]